ORIGINAL PAPER

J. M. Skowroński · A. Ważny

Nickel foam-based composite electrodes for electrooxidation of methanol

Abstract Nickel foam and five nickel foam-based composite electrodes were prepared for being used as anode materials for the electrooxidation of methanol in KOH solution containing 0.1 and 1.0 M of methanol. The layered electrodes composed of nickel foam, platinum nanoparticles, polyaniline (PANI) and/or porous carbon (C) prepared in various assemblies. As shown by SEM analysis, depending on the preparation conditions, the electrodes of different morphologies were obtained. Using the cyclic voltammetry method, the oxidation of methanol on nickel foam electrode was observed in the potential range 0.4 V ↔ 0.7 V, where the Ni(OH)$_2$/NiOOH transformation occurred. The presence of Pt particles in electrode gave rise to the increase in electrocatalytic activity in this potential range. For electrodes containing dispersed platinum catalyst (Ni/Pt, Ni/PANI/Pt and Ni/C/Pt), the oxidation of methanol was noted also in the potential range −0.5 V ↔ 0.1 V. The electrocatalytic activities of the examined electrodes toward methanol oxidation at low potentials were in order Ni/Pt > Ni/C/Pt > Ni/PANI/Pt, whereas at high potentials in order Ni/PANI/Pt > Ni/Pt > Ni/C/Pt > Ni. Among the examined electrodes, the most resistant to cyclic poisoning appeared to be the Ni/C/Pt electrode.

Keywords Methanol electrooxidation · Alkaline fuel cells · Nickel foam · Platinum · Polyaniline · Carbon

J. M. Skowroński (✉)
Poznań University of Technology,
Institute of Chemistry and Technical Electrochemistry,
ul. Piotrowo 3, 60-965 Poznań, Poland
E-mail: Jan.Skowronski@put.poznan.pl
Fax: +4861-665-2571

J. M. Skowroński · A. Ważny
Central Laboratory of Batteries and Cells, ul. Forteczna 12,
61-362 Poznań, Poland

Introduction

At present, in many research centres extensive work is being carried out on new types of electrode materials with possible practical application in alkaline fuel cells. One of the directions of research is focused on enhancing the efficiency of methanol oxidation. In the electrochemical oxidation of methanol, the electrode material is clearly an important parameter where a highly efficient and stable electrocatalyst is needed [1].

Inexpensive, easily available, conveniently transported, stored and easily-refuelled methanol is considered as an attractive liquid fuel for direct fuel cells [2–5] mainly due to the fact that methanol has a high energy density. The process of methanol oxidation to carbon dioxide occurs through a six-electron reaction [6]:

$$CH_3OH + H_2O = CO_2 + 6H^+_{aq} + 6e^-. \qquad (1)$$
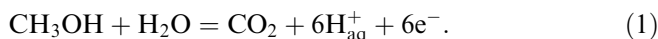
Platinum has been recognized as an important electrocatalyst in direct oxidation of small organic compounds, which may be used as a fuel, e.g. methanol [7]. For practical application, an acidic electrolyte is generally preferred and most research on platinum-based electrocatalysts for fuel cell electrodes has focused on catalysis in acidic media. One of the reasons for such a situation is the progressive carbonation with CO_2, which has brought about less interest in investigation of methanol oxidation in alkaline media. On the other hand, hydrogen ions are the product of the process of methanol oxidation Eq. 1 and the reaction equilibrium is shifted to the right in alkaline solution. Moreover during the oxidation of methanol in acidic solutions, the reaction intermediate, carbon monoxide, binds strongly to the catalyst surface and blocks the active sites [2]. In particular, pure Pt catalyst is sensitive to this poisoning effect. That effect can be mitigated, but not eliminated, through the incorporation of other metals and the use of alkaline media may be a promising avenue toward increased catalytic activity by well-balanced co-adsorption of methanol and the OH$^-$ ions at low potentials in an
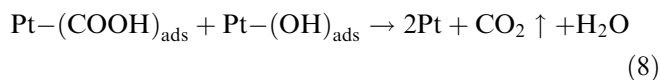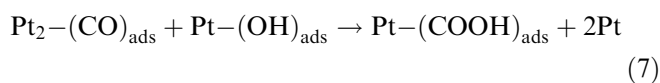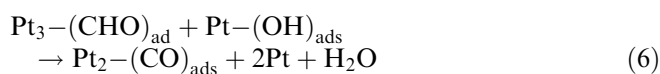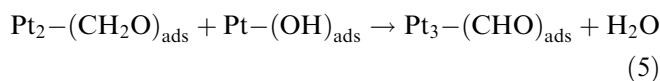
alkaline solution. Some studies of methanol oxidation on Pt in alkaline media, which have demonstrated a higher activity for methanol oxidation than in acid media are to be noted [8–13]. Low-temperature direct oxidation fuel cells that employ an alkaline electrolyte, possess clear kinetic advantages over acid fuel cells. Markovic et al. [14] have attributed the improved anode performance to higher surface OH^- coverage, resulting in the oxidation of adsorbed CO at lower potentials. Parsons and Noot [2] and also Nishimura et al. [15] found that the use of alkaline solutions in fuel cell has many advantages, such as increasing its efficiency. Tripkovic et al. [16] showed that in alkaline solution, smaller or negligible poisoning effects were observed. Consequently, the kinetic studies of methanol oxidation in alkaline solutions at different Pt-based catalysts may provide valuable data for the development of new, powerful catalysts.

Although the anodic process of methanol oxidation has been studied extensively over many years, the mechanism of the reaction is still under discussion [6, 8, 17–21]. There are many mechanisms proposed for methanol oxidation in alkaline medium. One path of this process is presented below [8]:

$$Pt + OH^- \Leftrightarrow Pt - (OH)_{ads} + e^- \tag{2}$$

$$2Pt + CH_3OH \Leftrightarrow PtH + Pt - (CH_3O)_{ads} \tag{3}$$

$$Pt-(CH_3O)_{ads} + Pt-(OH)_{ads} \rightarrow Pt_2-(CH_2O)_{ads} + H_2O \tag{4}$$

$$Pt_2-(CH_2O)_{ads} + Pt-(OH)_{ads} \rightarrow Pt_3-(CHO)_{ads} + H_2O \tag{5}$$

$$Pt_3-(CHO)_{ad} + Pt-(OH)_{ads} \rightarrow Pt_2-(CO)_{ads} + 2Pt + H_2O \tag{6}$$

$$Pt_2-(CO)_{ads} + Pt-(OH)_{ads} \rightarrow Pt-(COOH)_{ads} + 2Pt \tag{7}$$

$$Pt-(COOH)_{ads} + Pt-(OH)_{ads} \rightarrow 2Pt + CO_2 \uparrow + H_2O \tag{8}$$
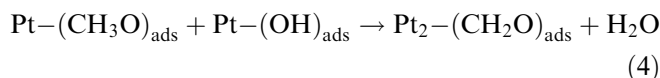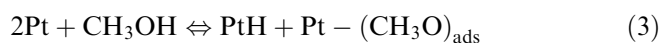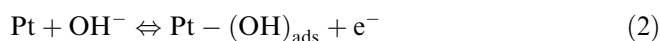
One of the impeding problems in the commercialisation in DMFCs is perhaps the high overpotential associated with the direct electrooxidation of methanol [22]. Additionally, the high cost of platinum limits its use. Thus, great effort has been devoted to the development of fuel cell electrocatalysts with the aims of increasing their activity, their tolerance toward poisoning by intermediate species occurring in the oxidation process and reducing the amount of noble metal used [23]. The electrocatalytic activity of platinum particles is known to depend greatly on their dispersity and surface properties [24–26] and consequently on the preparation method and supporting materials used [27]. A high degree of dispersion as well as a large surface area is desirable also for lowering the amount of noble metal, which is necessary for the cost reduction [28]. Therefore a great deal of interest has recently been concentrated on the choice of materials cheaper than platinum [29, 30] while maintaining high catalytic activity [28, 31–33].

Many electrodes involving nickel as a component in their manufacture can be used as a catalyst in fuel cells [34]. El-Shafei [35] examined the reaction of methanol oxidation on a nickel/glassy carbon composite electrode, whereas Rahim et al. [36] studied this reaction on a nickel/graphite composite electrode. The results reported in both papers led to the conclusion that methanol is oxidized with the participation of trivalent nickel after nickel is anodically oxidized to NiOOH. From electrochemical measurements Rahim et al. [29] concluded that methanol oxidation on the modified C/Ni-Ru electrode also begins at the potential value of the NiOOH formation with the creation of intermediate species. Skowroński and Ważny have previously found nickel foam, a lightweight and high porous (above 95%) material, to have a catalytic activity for methanol oxidation in alkaline solutions due to its surface oxidation properties [37]. For this reason, in the present work, nickel foam was used as a catalyst as well as catalyst-support during studies of methanol oxidation in alkaline electrolytes on new composite anodes.

In recent years, the intensive investigations on new types of electrode materials, electronically conducting polymers, have been developed concerning the possibility of their wide practical application [38]. Electrocatalytic oxidation of methanol with the use of conducting polymer and dispersed metal composites is probably the most explored process, obviously because of the possible application of these systems in fuel cells [39]. Polyaniline (PANI), which can be prepared through easy chemical and electrochemical synthetic routes and is air-stable for convenient handling, attracts more interest than the other polymers of this class [40]. The most important reason for incorporating platinum particles dispersed into a polyaniline matrix is to increase the specific area of these materials and thus improve catalytic efficiency [41]. The second reason is higher tolerance toward poisoning by intermediate species occurring in the oxidation process, in comparison with the serious problem of the poisoning effect on pure platinum electrodes.

Numerous publications have been devoted to carbon material used as catalytic support which exerts an important influence on fuel cell efficiency. The methods of preparation of the Pt nanoparticles and less expensive alloy nanoparticles, e.g., Pt/Ni, Pt/Ru/Ni [42] on the carbon support have attracted much interest in view of their superior electrocatalytic activity for fuel cell applications [29, 30, 43–48]. Because of their interesting properties, nanometer size and high surface area, carbon materials have been receiving increasing attention in recent years for their application as catalyst support for methanol oxidation [49–51].

The purpose of the present study was to make an attempt to prepare various types of nickel foam-based

composite catalysts for methanol oxidation, containing platinum particles dispersed (1) directly on nickel substrate, (2) in PANI matrix deposited on nickel substrate, (3) on nickel substrate followed by covering with carbon layer produced by heat treatment of PANI film deposited, (4) on carbon layer produced on nickel substrate by heat treatment of PANI film. In this paper, we show the results of our preliminary studies of the electrocatalytic properties of these nickel-based composite electrodes discussed from the point of view of individual and synergistic effects of the electrode constituents.

Experimental

All electrochemical measurements were carried out in a three-electrode system with a potentiostat-galvanostat PGSTAT30 Autolab (EcoChemieB.V.). The working electrodes were made of materials depicted in Table 1. Nickel foam (Fig. 1a) with thickness 1.6 mm, density 500 g/m^2 and porosity higher than 95% (produced by Nitech) was modified to prepare these electrodes. The geometrical area of all the electrodes was 1 cm^2. The counter electrode was the nickel sintered electrode filled with cadmium hydroxide. As the reference electrode was employed the Hg/HgO/6 MKOH system ($E = +0.098$ V vs. SHE; standard hydrogen electrode). The electrolyte was 6 M KOH solution either without or with CH$_3$OH (0.1 M or 1 M). Catalytic activity of all the electrodes in the reaction of methanol oxidation was measured by cyclic voltammetry (CV) method in the potential range $-0.65 \leftrightarrow 0.7$ V at a scan rate of 50 mV/s. All measurements were performed in unstirred electrolyte at a temperature of 20 °C. Using the CV technique, some nickel foam electrodes were coated with polyaniline film (Ni/PANI) (Fig. 1b) at a temperature of 25 °C. Deposition of polyaniline on various substrates was made in freshly prepared solution composed of 0.1 M H$_2$SO$_4$ + 0.1 M aniline, purged with argon to remove oxygen. For each electrode, twenty-five oxidation/reduction cycles were made in the potential range: -0.66 V $\leftrightarrow$ 0.50 V versus Hg/Hg$_2$SO$_4$/1M H$_2$SO$_4$ ($E = +0.674$ V vs. NEW) at a scan rate of 10 mV/s. Lead sheet was used as a counter electrode.

The platinum particles were dispersed on nickel foam (Ni/Pt) and on/in PANI film (Ni/PANI/Pt) (Fig. 1c) by galvanostatic reduction of chloroplatinic acid (0.03%) in 0.1 M H$_2$SO$_4$ for 2 h at current density of 1 mA/cm^2. Some electrodes were modified by heat treatment in

Table 1 A list of examined nickel-based composite electrodes

Electrode symbol	Electrode composition
Ni	Nickel foam
Ni/Pt	Nickel/platinum
Ni/PANI/Pt	Nickel/polyaniline/platinum
Ni/C	Nickel/carbon
Ni/Pt/C	Nickel/platinum/carbon
Ni/C/Pt	Nickel/carbon/platinum

argon, starting at room temperature with a heating rate of 20 °C/min upto 500 °C. The electrode were kept at this temperature for 5 min. In such a way three types of the carbon-coated electrodes were obtained. Thermal treatment of the Ni/PANI composite electrode resulted in Ni/C composite (Fig. 1d), whereas the Ni/Pt/PANI composite electrode was transformed into Ni/Pt/C composite due to heat treatment. Electrochemical deposition of platinum on the surface of Ni/C electrode provided Ni/C/Pt composite (Fig. 1e). Prior to deposition of Pt particles, some Ni/Pt and Ni/C/Pt electrodes were potentially cycled in the region of hydrogen evolution in methanol-free KOH. This treatment was made according to the following procedure. Starting from the rest potential of electrode with a scan rate 0.1 mV/s, the potential was changed in the positive direction to reach -0.05 V and after the reversal of polarization the potential was reduced until the cathodic current of 4 mV was attained. At this moment the direction of polarization was again reversed and the potential sweep was terminated at the starting potential.

For observing the morphological changes of electrodes resulting from the electrochemical and thermal treatment the scanning electron microscopy (SEM) analysis was carried out using a Tescan-Vega 5135 with the acceleration voltage of 15 kV.
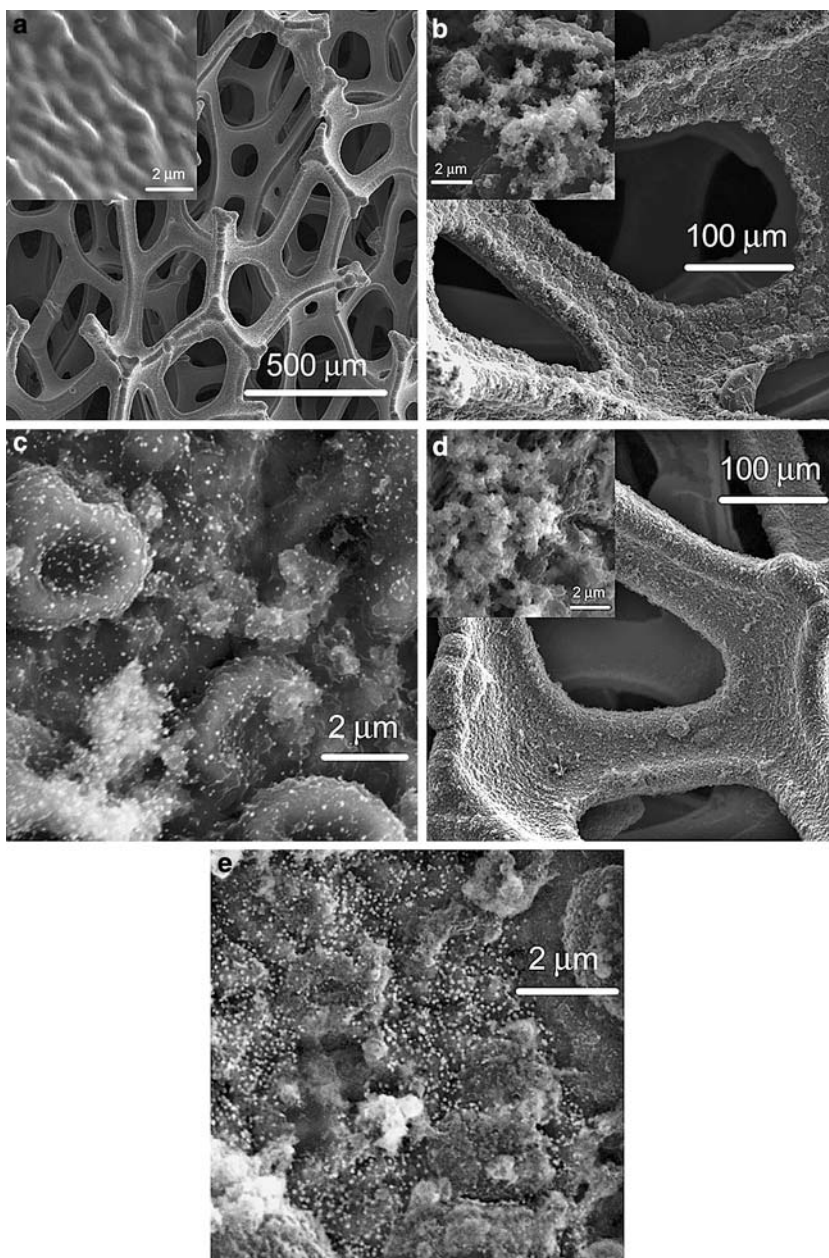
Results and discussion

Figure 1a shows SEM micrographs for nickel foam. As seen from this Figure, the nickel skeleton is composed of holed cells linked to each other. The arch ribs of these cells with sharp edges are non-porous. Only grain boundaries are visible at a high magnification (see inset). CV curves recorded in 6 M KOH for nickel foam electrode are shown in Fig. 2. During the forward sweep, starting at the rest potential of electrode, an asymmetric anodic peak (A$_2$), associated with the oxidation reaction β-Ni(OH)$_2$ → (β,γ)-NiOOH [36, 37, 52–56], is recorded at the potential of about 0.4 V. This peak is responded by cathodic peak appearing at 0.3 V during the backward sweep. During the following cycles, peak A$_2$ splits into two peaks, due to the formation of two forms of NiOOH, β and γ and, an increase in the peak current takes place.

After addition of 0.1 M methanol to KOH solution (Fig. 3), only a small anodic peak A$_2$ is recorded in the first cycle at the potential corresponding to the β-Ni(OH)$_2$ → (β,γ)-NiOOH transformation. On increasing the potential further, the peak current raises violently to form a broad peak A$_3$ at about 0.6 V, which is responded by an anodic peak a$_3$, corresponding to the reactivation of the catalytic sites present on the electrode surface. Both these effects are indicative of the oxidation of methanol catalyzed by Ni(III) ions present in NiOOH formed at the nickel foam surface [37, 53, 57, 58]. In the next cycles, peak A$_3$ becomes much more shaped (CV

Fig. 1 SEM micrographs for nickel foam (**a**), Ni/PANI (**b**), Ni/PANI/Pt (**c**), Ni/C (**d**), Ni/C/Pt (**e**)

curve for the tenth cycle is presented in Fig. 3). For the tenth cycle, a sharp and relatively high peak A_2 is responded by proportionally higher cathodic peak. This result means that the amount of Ni(III) on the Ni electrode increases upon cycling. Simultaneously, the electrocatalytic activity towards methanol oxidation decreases a little (the decrease in peak A_3). One of the reasons, which should be concerned, to elucidate such behavior is an exhaustion of methanol at the electrode/electrolyte interface upon cycling. This reason has its origin in both a low concentration of methanol in KOH solution and the difficulty in methanol transportation from the bulk of electrolyte to the electrode surface in an unstirred solution.

The electrocatalytic activity of the electrode toward methanol oxidation considerably increases in the above-mentioned potential range (about twofold higher intensity of peak A_3) for Ni/Pt electrode (solid line in Fig. 4). This increase can be attributed to the catalytic action of Pt particles dispersed on the nickel surface. The anodic peak appearing during the forward sweep followed by the reactivation anodic peak during the backward sweep have been previously found, in the potential range close to that discussed here, for the reaction of methanol oxidation occurring on smooth Pt foil and on porous unsupported Pt electrodes in 6 M KOH [17]. As compared to Ni/Pt electrode, much higher peak A_3 is observed in Fig. 4 for a sandwich-like electrode consisting of three layers: Ni/PANI/Pt (dashed line) (Table 1). The increase in current density of peak A_3 occurs in parallel with the increase in both the anodic peak A_2, corresponding to the oxidation reaction
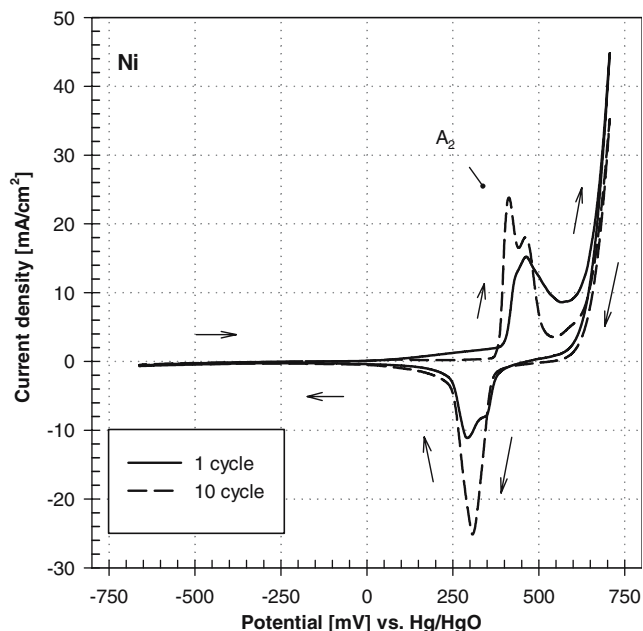
Fig. 2 Cyclic voltammograms recorded in 6 M KOH for nickel foam electrode. Scan rate: 50 mV/s. Potential range: −0.65 V↔0.70 V versus Hg/HgO/6M KOH

Fig. 4 Cyclic voltammograms (1st cycle) recorded for methanol oxidation on Ni/Pt electrode (*solid line*) and Ni/PANI/Pt electrode (*dashed line*) in 6 M KOH containing 0.1 M CH_3OH. Scan rate: 50 mV/s. Potential range: −0.65 V ↔ 0.70 V
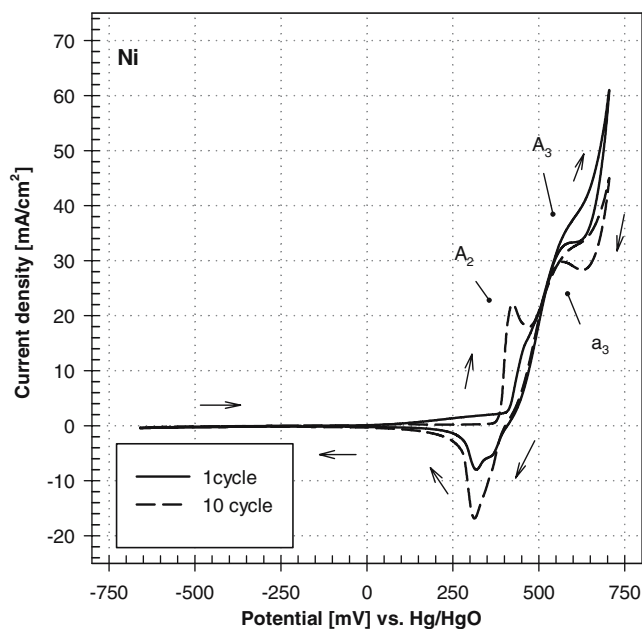

Fig. 3 Cyclic voltammograms recorded for methanol oxidation on nickel foam electrode in 6 M KOH containing 0.1 M CH_3OH. Scan rate: 50 mV/s. Potential range: −0.65 V↔0.70 V versus Hg/HgO/6M KOH

$Ni(OH)_2 \rightarrow NiOOH$, and the cathodic response from this reaction on the backward sweep. The existence of the peaks arising from methanol oxidation promoted by Ni(III) ions show that PANI film is sufficiently porous to make the diffusion of both the OH^- ions and methanol molecules to the nickel surface possible. A better
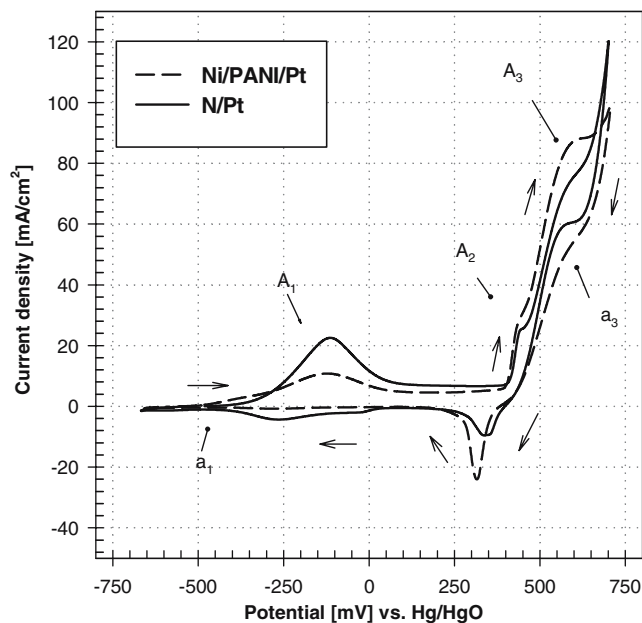
electrocatalytic activity of Ni/PANI/Pt electrode in the potential range 0.4 V ↔ 0.7 V indicates that Pt nanoparticles are dispersed not only on the porous PANI surface (Fig. 1c) but also in the PANI interior down to the PANI/Ni interface. It is likely that the Pt-Ni interaction on the nickel foam surface is responsible for a higher efficiency of the $Ni(OH)_2 \rightarrow NiOOH$ transformation. Due to this reaction occurring on the Ni surface, the Ni-Pt sites change into NiOOH-Pt ones. Apart from the peaks observed in Fig. 4 in the potential range 0.4 V ↔ 0.7 V, a new pair of peaks (A_1-a_1), associated with the oxidation of methanol, is recorded for the Ni/Pt and Ni/PANI/Pt electrodes in the potential range −0.5 V ↔ 0.1 V. Because in this potential range, NiOOH does not exist due to the precedent reduction occurring during the negative scan, the restored Ni-Pt sites take part in the reaction of methanol oxidation. As seen from Fig. 3, peaks (A_1-a_1) do not appear in this potential range for platinum-free electrodes. From this discussion one can infer that in the case of nickel foam-based electrodes coated with dispersed Pt, the process of methanol oxidation develops consecutively in two potential ranges involving the reaction occurring at low potentials with the assistance of Ni-Pt catalyst (peak A_1) and the reaction catalyzed by NiOOH-Pt at high potentials (peak A_3). The peaks positioned at low potentials have been recently reported for the oxidation of methanol taking place in alkaline solutions at the carbon-supported Co-Pt nanoparticles [51] and carbon-supported Au-Pt nanoparticle catalysts [59]. The peaks (A_1-a_1) in Fig. 4 are higher for Ni/Pt (solid line) than for a ternary Ni/PANI/Pt (dashed line), in which Pt particles are dispersed on/in the PANI matrix coating the nickel surface

(Fig. 1c). This result seems to be striking in the light of fact that the latter electrode is more active in the oxidation reaction of methanol occurring at high potentials within the peaks (A₃-a₃). This discrepancy vanishes, however, if it is distinguished that different catalytic sites, Ni-Pt existing in a low potential range and NiO-OH-Pt existing in a high potential range, are involved in the reactions corresponding to peaks A_1 and A_3, respectively.

CV curves recorded for electrodes modified in such a way that PANI film was transformed into carbon layer due to heat treatment are shown in Fig. 5. As seen from this Figure, carbon layer coating the nickel surface of Ni/C electrode results in almost complete inactivation of nickel toward methanol oxidation (dashed line). Similar effect is observed for Ni/Pt/C electrode, in which Pt particles are sandwiched between nickel substrate and carbonized layer of polyaniline (solid line). The morphology of the nickel surface coated with carbon layer is shown in Fig. 1d. As can be seen from the image recorded at a higher magnification (see inset in Fig. 5), the outer surface of carbon layer is porous. This observation must not mean that some metal surface is unoccupied by carbon, because carbon sponge could grow on the thin and nonporous carbon layer strictly adhering to metal. In such a case the loss of electrocatalytic activity of Ni and Pt in Ni/C and Ni/Pt/C composite, respectively, can be interpreted assuming that a tight carbon layer makes an access of electrolyte to the metal surface impossible. For electrodes not completely coated with carbon layer
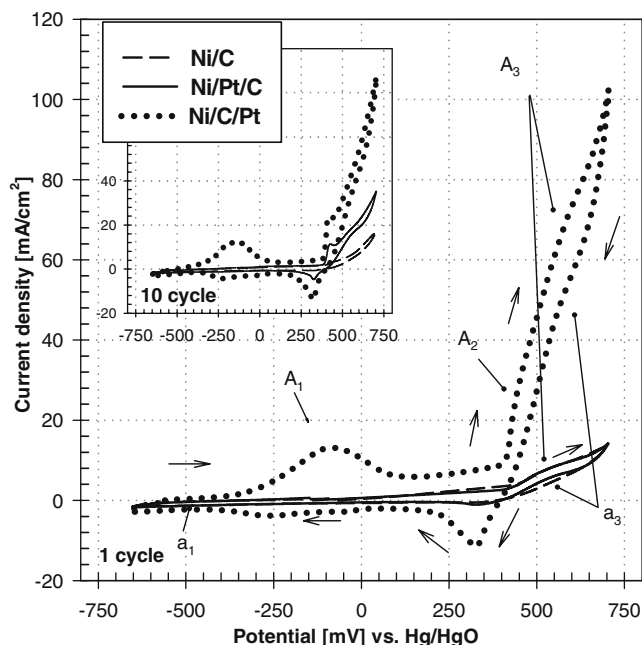

Fig. 5 Cyclic voltammograms recorded for methanol oxidation on Ni/Pt/C electrode (*solid line*), Ni/C electrode (*dashed line*) and Ni/C/Pt electrode (*dotted line*). Scan rate: 50 mV/s. Potential range: −0.65 V ↔ 0.70 V

their inactivation might be ascribed to the gas products evolved during the carbonization process of PANI, which are adsorbed at the Ni and Ni-Pt sites resulting in their poisoning. The poisoning of catalysts in fuel cells by CO is well known. For the tenth cycle a considerable increase in current density of Ni/Pt/C and only a small increase of Ni/C electrode were noted in the potential range 0.4 V ↔ 0.7 V (see inset in Fig. 5). This feature shows that the Ni electrode onto which platinum particles are deposited is much more effectively reactivated. In contrast to Ni/C and Ni/Pt/C electrodes, Ni/C/Pt electrode exhibits a high electrocatalytic activity in the reaction of methanol oxidation. It is worth noting that for this electrode Pt particles were deposited on a porous carbon layer covering the nickel foam surface (dotted line in Fig. 5). This electrode is active not only in the potential range 0.4 V ↔ 0.7 V, where the reaction is catalyzed by Ni(III) but also in the potential range −0.5 V ↔ 0.1 V, where the reaction is controlled by Ni-Pt catalysts. It suggests that during the cathodic process of Pt deposition on the carbon surface, Ni sites coated with carbon film are uncovered. In contrast to Ni/C/Pt, for Ni/Pt/C no anodic peak is recorded at about −0.1 V. The lack of this peak proves that in the latter electrode Pt particles cannot take into reaction with methanol because they are encapsulated in a tight and non-porous carbon shell. The problem of the electrochemical reactivation of catalyst by the cathodic treatment is discussed below.

As can be seen from Fig. 6, Ni/Pt/C electrode is the only one, which upon cycling demonstrates an increasing catalytic activity in the potential range 0.5 V ↔ 0.7 V. Concerning the electrocatalytic behavior of Ni/C/Pt electrode, in which Pt particles are present on/in carbon layer instead under this layer (as for Ni/Pt/C electrode), one can notice that in comparison with the best Ni/Pt and Ni/PANI/Pt electrodes in the potential range 0.5 V ↔ 0.7 V, the electrocatalytic activity of Ni/C/Pt electrode is a little worse in the first cycle but is significantly better in the tenth cycle. This result indicates that there is an access of methanol to Ni sites. Ni/C/Pt electrode is the most resistant against the cyclic poisoning among all the examined electrodes. Such a behavior may be related to a porous structure of the carbon layer, which enables both a fast transportation of methanol-admixed electrolyte to the nickel surface and homogeneous dispersing of Pt nanoparticle catalyst on porous carbon surface (Fig. 1e). From comparison of Figs. 5 and 4, the conclusion can be drawn that Ni/C/Pt electrode is more active toward methanol oxidation in the potential range −0.5 V ↔ 0.1 V than electrode Ni/PANI/Pt but less active than electrode Ni/Pt (Table 2). Tentative explanation for the best electrocatalytic activity of Ni/Pt electrode may be synergic interaction of Pt particle with Ni sites on the nickel foam surface. The improvement of the electrocatalytic activity of platinum nanoparticles in the reaction of methanol oxidation due to synergic effect has been

Fig. 6 Effectiveness of various electrodes in the reaction of methanol oxidation estimated by comparison of anodic charges calculated based on CV curves recorded in (Figs. 1, 2, 3). Potential range: 0.5 V ↔ 0.70 V
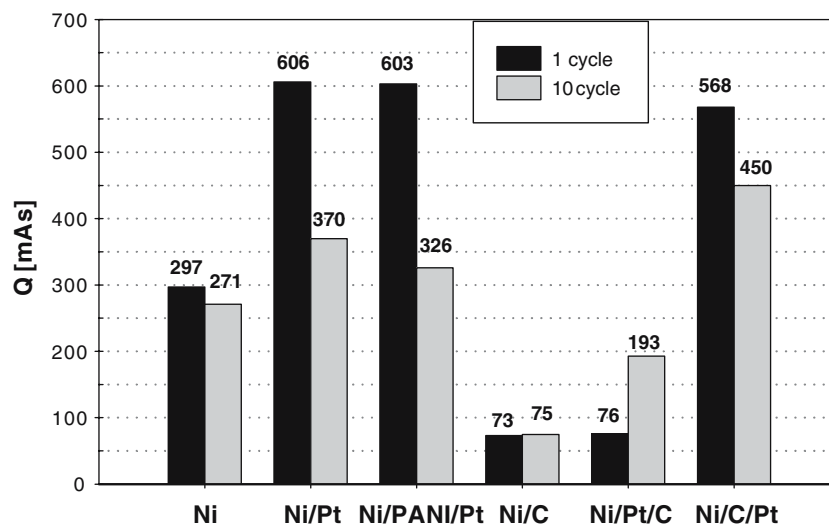
Table 2 Electrochemical data measured based on cyclic voltammograms for various types of nickel-based composite electrodes recorded in 6 M KOH containing 0.1 M CH₃OH

Electrode symbol	Cycle number	A₁-forward scan		A₂-forward scan		A₃-forward scan		a₃-backward scan	
		Peak potential, E (mV)	Peak current, i (mA/cm²)	Peak potential, E (mV)	Peak current, i (mA/cm²)	Peak potential, E (mV)	Peak current, i (mA/cm²)	Peak potential, E (mV)	Peak current, i (mA/cm²)
Ni	1	–	–	458	14.5	590	36.2	559	31.6
	10	–	–	430	21.7	590	31.9	550	29
Ni/Pt	1	−109	22.5	440	24.7	590	74.1	561	58.4
	10	−192	16.3	422	38.3	590	42.8	542	33.1
Ni/PANI/Pt	1	−126	10.8	432	26	590	87.1	578	50.7
	10	−191	3	413	36.4	590	44.5	560	25.9
Ni/C	1	–	–	–	–	590	9.7	–	13.8
	10	–	–	–	–	590	8.3	–	15.1
Ni//Pt/C	1	–	–	–	–	590	9.7	540	5.7
	10	–	–	430	11.4	590	21.5	558	16
Ni/C/Pt	1	−85	13.2	445	27.1	590	72	576	47.7
	10	−132	12.3	427	22.8	590	52.1	576	38.9

recently reported for carbon-supported bimetallic Co-Pt [51] and Au-Pt [59] catalysts. It is interesting to note that the electroactivity of Ni/Pt electrode (expressed as the anodic peak current; see Table 2) is 70% higher in the first cycle and only 30% higher in the tenth cycle as compared to that of Ni/C/Pt electrode. On the other hand, cyclic inactivation proceeds the most rapidly for Ni/PANI/Pt electrode. This fact may be related to chemical degradation of polyaniline layer at high potentials.

Figure 7 presents the influence of the methanol concentration on the kinetics of the oxidation reaction of methanol for the Ni/Pt and Ni/C/Pt electrodes. A particular attention in this Figure is paid to the reaction proceeding in low potential range. From a comparison of CV curves recorded in the electrolyte containing 0.1 M (curves (a') and (b') presented in insets) and 1.0 M (curves a and b) of methanol, it is clear that the

reaction rate of both electrodes considerably increases for higher concentration of methanol. However, the increase in anodic peak positioned at about −0.1 V is much more marked for Ni/Pt electrode (20-fold increase in the first cycle; solid line) than for Ni/C/Pt electrode (tenfold increase in the first cycle; dashed line). A characteristic property of the curves recorded in 6 M KOH admixed with 1 M methanol is the appearance of distinctly pronounced anodic peak at about −0.35 V during the backward sweep. The existence of this peak is generally accepted as an evidence for the occurrence of methanol oxidation on the reactivated catalyst surface. In the tenth cycle a shoulder appears at the left side of the anodic peak during the forward sweep. This feature can be related to bi-functional performance of Ni/Pt catalyst arising from the contribution of electrocatalytic activity of each component to the oxidation reaction of methanol.
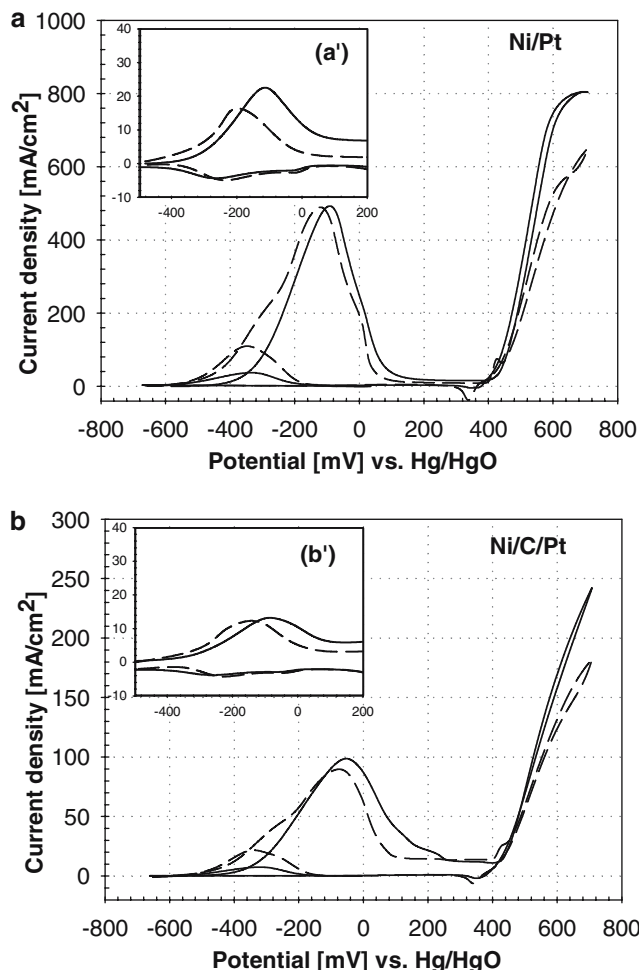
Fig. 7 Cyclic voltammograms recorded for methanol oxidation on nickel-based composite electrodes in 6 M KOH containing 1.0 M CH₃OH (**a**), (**b**) and in 6 M KOH containing 0.1 M CH₃OH (**a′**), (**b′**). Scan rate: 50 mV/s. Potential range: −0.65 V ↔ 0.70 V. Cycle 1 (*solid line*), cycle 10 (*dashed line*)

Fig. 8 Cyclic voltammograms recorded for methanol oxidation on **a** Ni/Pt electrode, **b** Ni/C/Pt electrode exposed to cathodic treatment prior to Pt deposition, **c** Ni/C/Pt electrode in 6 M KOH containing 0.1 M CH₃OH. Scan rate: 50 mV/s. Potential range: −0.65 V ↔ 0.70 V

The effect of cathodic treatment of nickel foam and Ni/C composite, prior to the Pt deposition, on the activity of Ni/Pt and Ni/C/Pt electrodes in the reaction of methanol oxidation is shown in Fig. 8. This treatment associated with hydrogen sorption exerts no influence on the electrocatalytic activity of Ni/Pt electrode, whereas the activity of the cathodically-treated Ni/C/Pt (dashed line) is 1.8 times higher as compared to untreated electrode (dotted line). This improvement might be attributed to the following effects: (a) the reduction of a non-conductive passive layer existing between the nickel surface and adjacent carbon layer, (b) the removal of surface functional groups from the carbon surface resulting in enhanced activity of the carbon-supported Pt sites, (c) the development of the carbon layer porosity, via the opening of pores, allowing an easier penetration of both the $PtCl_6^{2-}$ ions to the nickel surface to form a binary Ni-Pt sites upon electrochemical deposition, and methanol molecules to these sites in the course of its electrooxidation.
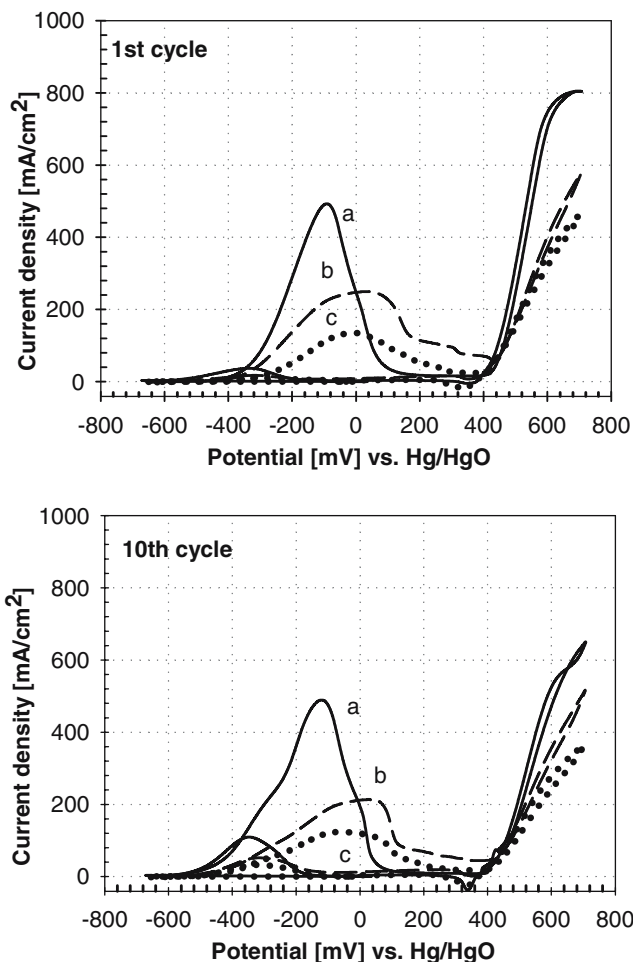
Conclusions

The reaction of methanol oxidation in alkaline solution was studied by cyclic voltammetry using a series of new nickel foam based composite electrodes. It was shown that the process at nickel foam electrode occurs via the oxidation reaction $Ni(OH)_2 \rightarrow NiOOH$ in the potential range 0.5–0.7 V. The electrocatalytic activity of the electrode toward methanol oxidation increases significantly after dispersing the platinum nanoparticles on the nickel surface. For this electrode, the second region of methanol oxidation was also revealed at low potentials ranging between −0.5 V and 0.1 V. The reaction taking place in this potential range can be related to the first step of methanol oxidation at the Pt nanoparticles. However, to explain in detail the mechanism of a two-step reaction of methanol oxidation further investigations are needed. The oxidation of methanol in the two zones was also observed for the Ni/PANI/Pt and Ni/C/Pt composite electrodes. The character of CV curves

suggests that the Ni-Pt and NiOOH-Pt interactions can play a role in determining the electrocatalytic activity of the composite electrodes in the low and high potential range, respectively.

In the first cycle, the electrocatalytic activities of the examined electrodes toward methanol oxidation in the potential range -0.5 V $\leftrightarrow$ 0.1 V are in order Ni/Pt > Ni/C/Pt > Ni/PANI/Pt, whereas in the potential range 0.5 V $\leftrightarrow$ 0.7 V in order Ni/Pt > Ni/PANI/Pt > Ni/C/Pt > Ni. Among the examined electrodes, the most resistant to cyclic inactivation appeared to be Ni/C/Pt electrode. After ten cycles the loss in activity for this electrode was 7.3%, whereas for Ni/Pt electrode (the most active electrode in the first cycle) it was 38.0%. It is worth noting that for a long-term cyclic oxidation of methanol, the Ni/Pt/C electrode demonstrated the most pronounced increase in activity. Its anodic charge changed from 193 mAs for the tenth cycle to 284 mAs for the hundredth cycle. Despite such an improvement, the latter value was still lower than that of the Ni/C/Pt electrode; 383 mAs.

All the examined electrodes exhibited enhanced electrocatalytic activity on increasing the methanol concentration in KOH solution. The increase in activity varied depending on the type of electrode. For example, the anodic peak current at about -0.1 V increased 19.8 times for the Ni/Pt electrode and 7.6 times for Ni/C/Pt electrode as the methanol concentration changed from 0.1 M to 1.0 M.

The preliminary studies showed that the electrocatalytic activity of Ni/C/Pt catalyst can be improved if the binary Ni/C electrode is electrochemically treated in the region of hydrogen sorption followed by the deposition of Pt nanoparticles on the modified carbon surface. The results of measurements not reported here show that the effectiveness of such a treatment depends on the experimental conditions (e.g., the potential of hydrogen evolution, the number of cycles and the cycling mode). Based on this, one can expect further improvement of the catalyst activity owing to the optimization of this method.

References

 1. Sasaki K, Wang JX, Balasubramanian M, McBreen J, Uribe F, Adzic RR (2004) Electrochim Acta 49:3873
 2. Parson R, VaderNoot T (1988) J Electroanal Chem 257:9
 3. Grug BN, Marcovic NM, Ross PN (1998) Electrochim Acta 43:3631
 4. Grug BN, Marcovic NM, Ross PN (1998) Phys Chem B 101:3910
 5. Ren X, Zelenay P, Thomas S, Davey J, Gottesfeld S (2000) J Power Sources 86:73
 6. Love JG, Brooksby PA, McQuillan AJ (1999) J Electroanal Chem 464:93
 7. Herrero E, Fernandez-Vega A, Feliu JM, Adlaz A (1993) J Electroanal Chem350:73
 8. Beden B, Kadirgan F, Lany C, Leger JM (1982) J Electroanal Chem 142:171
 9. Caram JA, Gutierrez C (1992) J Electroanal Chem 323:213
10. Perez JM, Munoz E, Morallon E, Cases F, Vazquez JL, Aldaz A (1994) J Electroanal Chem 368:285
11. Prabhuram J, Manoharan R (1998) J Power Sources 74:54
12. McLean GF, Niet T, Prince-Richard S, Djilali N (2002) Int J Hydrogen Energy 27:507
13. Yu EH, Scott K, Reeve RW (2003) J Electroanal Chem 547:17
14. Markovic NM, Schmidt TJ, Grgur BN, Gasteiger HA, Behm RJ, Ross PN (1999) J Phys Chem B 103:8568
15. Nishimura K, Machida K, Enyo M (1988) J Electroanal Chem 251:117
16. Tripkovic AV, Marinkovic N, Popovic KDj, Adzic RR (1995) Russ J Electrochem 31:993
17. Manoharan R, Prabhuram J (2001) J Power Sources 96:60
18. Acress GJK (2001) J Power Sources 100:60
19. Borkowska Z, Tymosiak-Zielińska A, Shul G (2004) Electrochim Acta 49:120
20. Spendelow JS, Lu GQ, Kenis PJA, Wieckowski A (2004) J Electroanal Chem 568:215
21. Tripković AV, Popović KDj, Lović JD, Jovanović VM, Kowal A (2004) J Electroanal Chem 572:119
22. Burstein GT, Barnett CJ, Kucernak AR, Williams KR (1997) Catal Today 38:425
23. Manoharan R, Prabhuram J (2001) J Power Sources 96:220
24. Katsuaki S, Kohei U, Hideaki K, Yoshinobu N (1988) J Electroanal Chem 256:481
25. Watanabe M, Saegusa S, Stonehart P (1989) J Electroanal Chem 271:213
26. Katsuaki S, Ryuhei I, Hideaki K (1990) J Electroanal Chem 284:523
27. Yano J, Ogura K, Kitani A, Sasaki K (1992) Synth Met 52:21
28. Gloaguen F, Leger JM, Lamy C (1997) J Appl Electrochem 27:1052
29. Abdel Rahim MA, Abdel Hameed RM, Khalil MW (2004) J Power Sources 135:42
30. Kuk ST, Wieckowski A (2005) J Power Sources 141:1
31. Greszczuk M (1994) Electrochim Acta 39:1809
32. Prasad KR, Munichandraiah N (2001) Synth Met 123:459
33. Prasad KR, Munichandraiah N (2002) Synth Met 130:17
34. Lin S-M, Wen T-C (1995) J Appl Electrochem 25:73
35. El-Shafei A.A (1999) J Electroanal Chem 471:89
36. Abdel Rahim MA, Abdel Hameed RM, Khalil MW (2004) J Power Sources 134:160
37. Skowroński JM, Ważny A (2002) Mol Phys Rep 35:49
38. Malinauskas A(1999) Synth Met 107:75
39. Schultze JW, Karabulut H (2005) Electrochim Acta 50:1739
40. Aoki K, Tano S (2005) Electrochim Acta 50:1491
41. Niu L, Li Q, Wei F, Chen X, Wang H (2003) Synth Met 139:271
42. Park K-W, Choi J-H, Kwon B-K, Lee S-A, Sung Y-E, Ha H-Y, Hong S-A, Kim H, Wieckowski A (2003) J Phys Chem 107:5467
43. Biswas PC, Nodasaka Y, Enyo M (1996) J Appl Electrochem 26:30
44. Schmidt TJ, Noeske M, Gasteiger HA, Behm RJ, Britz P, Bonnemann H (1998) J Electrochem Soc 145:925
45. Wang X, Hsing I-M (2002) Electrochim Acta 47:2981
46. King WD, Corn JD, Murphy OJ, Boxall DL, Kenik EA, Kwiatkowski KC, Stock SR, Luckehart CM (2003) J Phys Chem B 107:5467
47. Spinace EV, Neto AO, Linardi M (2004) J Power Sources 129:121
48. Bhattacharya A, Hazra A,Chatterjee S, Sen P, Laha S, Basumallick I (2004) J Power Sources 136:208
49. He Z, Chen J, Liu D, Tang H, Deng W, Kuang Y (2004) Mater Chem Phys 85:396
50. Rodriguez-Nieto FJ, Morante-Catacora TY, Cabrera CR (2004) J Electroanal Chem 571:15
51. Zhang X, Tsang KY, Chan KY (2004) J Electroanal Chem 573:1
52. Bode H, Dehmelt K, Witte J (1961) Electrochim Acta 11:1079
53. Fleichmann M, Korinek K, Pletcher D (1971) J Electroanal Chem 31:39

54. Fleichmann M, Korinek K, Pletcher D (1972) J Chem Soc Perkin Trans II:1396
55. Hahn F, Beden B, Croissant MJ, Lamy C (1986) Electrochim Acta 31:335
56. Czerwiński A, Dmochowska M, Grdeń M, Kopczyk M, Wójcik G, Młynarek G, Kołata J, Skowroński JM (1999) J Power Sources 77:28
57. Enea O (1990) Electrochim Acta 35:375
58. Vukovic M (1994) J Appl Electrochem 24:878
59. Luo J, Maye MM, Kariuki NN, Wang L, Njoki P, Lin Y, Schadt M, Naslund HR, Zhong CJ (2005) Catalysis Today 99:291